Energy Conversion and Management 100 (2015) 232–241

Contents lists available at ScienceDirect

Energy Conversion and Management

journal homepage: www.elsevier.com/locate/enconman

Comparison study on combustion characteristics and emissions of a homogeneous charge compression ignition (HCCI) engine with and without pre-combustion chamber

Amin Yousefi [a,*], Ayatallah Gharehghani [a], Madjid Birouk [b]

[a] Department of Mechanical Engineering, Amirkabir University of Technology, 424 Hafez Avenue, P.O. Box 15875-4413, Tehran, Iran
[b] Department of Mechanical Engineering, University of Manitoba, Winnipeg, Manitoba R3T 5V6, Canada

ARTICLE INFO

Article history:
Received 4 March 2015
Accepted 8 May 2015
Available online 19 May 2015

Keywords:
Combustion chamber
Pre-chamber
HCCI combustion mode
Performance
Emissions

ABSTRACT

There is an urgent need to develop new combustion strategies such as homogeneous charge compression ignition (HCCI) mode to meet current and future emissions regulations. In this study, experiments and a coupled AVL-CHEMKIN CFD (computational fluid dynamic) model were adopted to compare combustion phasing, engine performance and emissions in term of equivalence ratio for both HCCI combustion engines with and without pre-combustion chamber to investigate the effect of pre-combustion chamber on HCCI combustion engine. Results revealed that with an equivalence ratio of 0.2, HCCI engine with pre-combustion chamber (comet MK.V) tolerates misfiring process, while HCCI engine without pre-combustion chamber (modified chamber) experiences a complete combustion. HCCI engine with modified chamber has higher combustion pressure, narrower heat release rate (HRR), more advanced start of combustion (SOC) and higher indicated mean effective pressure (IMEP) in comparison with comet MK.V chamber. For equivalence ratios between 0.2 and 0.5, the average increase in IMEPs is 49.3%. Furthermore, HCCI engine with modified chamber generates higher work per kg fuel compared to comet MK.V chamber. While a high level of nitrogen oxide (NO_x) emissions is produced by HCCI combustion with modified chamber, both carbon monoxide (CO) and hydrocarbon (HC) emissions decreased drastically. In terms of combustion phasing, engine performance and emissions, the HCCI engine with modified combustion chamber is preferred at low equivalence ratios ($\Phi < 0.3$) compared with comet MK.V chamber.

1. Introduction

HCCI combustion is a spontaneous multi-site combustion of a highly diluted air/fuel mixture characterized by rapid pressure rise and fast heat release. HCCI combustion is an alternative combustion mode, which has the potential of meeting low levels of NO_x and PM (particulate matter) emissions, while still achieving high thermal efficiency [1]. Apart from these favorable attributes of HCCI combustion, the control of auto-ignition is still a major obstacle for the implementation of HCCI technology in practical engines, which depends mostly on the heat release from chemical kinetics [2]. However, operating conditions such as initial pressure and temperature and compression ratio can also affect the chemical kinetics. One of the main parameters which impacts on the heat release is the intake air temperature. Increasing intake temperature advances the SOC but reduces the volumetric efficiency [3,4]. Aside from, increasing intake pressure rises the charge temperature during the compression stroke which affects HRR and it is helpful for enhancing ignition and combustion stability of HCCI engine, especially for leaner mixtures [5,6]. Variable compression ratio (VCR) [7–9] is another controlling method for HCCI combustion. The obvious effect of compression ratio is increasing HRR and advancing the ignition delay due to the higher pressure and temperature and overall reactivity. HRR can be affected by dilution with Exhaust gas recirculation (EGR) [10]. EGR retards the combustion phasing since it contains species with high specific heats (CO_2 and H_2O) which reduces the compression temperature [11]. Furthermore, using variable valve actuation (VVA) with valve timings set affects HRR in such way that different amount of swirl is provoked inside in the combustion chamber [12–14].

Combustion chamber geometry can also affect the HRR and combustion phasing in HCCI combustion engines. The role of

* Corresponding author. Tel.: +98 936 3847529.
E-mail addresses: a.yousefi@aut.ac.ir, amin_50@yahoo.com (A. Yousefi).

http://dx.doi.org/10.1016/j.enconman.2015.05.024
0196-8904/

Nomenclature

ABDC	after bottom dead center
ATDC	after top dead center
AFR	air fuel ratio
BDC	bottom dead center
BBDC	before bottom dead center
BTDC	before top dead center
CD	combustion duration
CI	compression ignition
CO	carbon monoxide
CAD	crank angle degree
CFD	computational fluid dynamic
EGR	exhaust gas recirculation
ER	equivalence ratio
EVC	exhaust valve close
EVO	exhaust valve open
HC	hydrocarbon
HCCI	homogeneous charge compression ignition
HRR	heat release rate
IC	internal combustion
IMEP	indicated mean effective pressure
IVC	inlet valve close
IVO	inlet valve open
NO_x	nitrogen oxide
MFB	mass fraction burnt
P	pressure
PM	particulate matter
rpm	revolution per minute
SOC	start of combustion
TDC	top dead center
V	volume
VCR	variable compression ratio
VVA	variable valve actuation

piston geometry in generating turbulence and thereby reducing the rate of heat release and increasing the combustion duration (CD) in HCCI mode has been investigated experimentally. Vressner et al. [9] studied the effect of combustion chamber geometry on a HCCI engine by using high speed chemiluminescence imaging where two different combustion chamber geometries were investigated; one with a disc shape and another with a square bowl in piston. Their results showed that a square bowl in the piston generates higher turbulence level, which consequently resulted in a significantly decreased HRR and increased CD. They also reported that the load can be increased using a square bowl in piston geometry since the pressure rise rate will be lower compared to disc geometry.

Christensen et al. [15] compared a high turbulent square bowl in a piston combustion chamber with a low turbulent disc combustion chamber. Their results revealed that the combustion chamber geometry plays an important role in HCCI combustion. At the same operating conditions, the peak combustion rate for the square bowl piston was found much lower compared to the disc shaped piston, which was attributed to larger heat losses, lower combustion efficiency and higher turbulence.

The influence of different combustion chamber configurations on HCCI combustion process with a single cylinder optical engine was investigated by Liu et al. [16]. They examined three combustion chamber geometries including V-type, H-type and A-type. Their results revealed that the high temperature auto-ignition occurred in the center of A-type combustion chamber, while it was more dispersive and closer to the chamber wall for the V-type configuration. Among these geometries HRR and pressure rise rate was the highest and CD was the shortest for the V-type combustion chamber, while the A-type combustion chamber, which induced higher turbulence intensity, resulted in a moderate pressure rise rate and HRR.

Yu et al. [17] employed two different piston shapes, a flat disc and a square bowl, to examine the effect of in-cylinder turbulence on the temperature field and combustion process in methanol fueled HCCI engine by generating different in-cylinder turbulence and temperature field prior to auto-ignition. Compared to the disc shaped piston, the square bowl has a higher temperature inhomogeneity owing to the turbulence wall heat transfer. Higher CD and slower pressure rise rate was achieved in the square bowl engine compared to the disc shaped bowl.

The influence of turbulence, through changes in swirl velocity and EGR, on the combustion process was investigated theoretically and experimentally in a HCCI engine by Espadafor et al. [18]. The combustion process in a high swirl bowl in piston has been compared to that is an almost flat shape. They concluded that, under same operating conditions, the peak of the HRR for the high swirl ratio piston was lower compared to the flat shape piston bowl. In addition, CD was increased, which is due to the reduction of gas temperature and larger heat losses.

As represented in the previous researches, it can be concluded that turbulence and swirl ratio plays a crucial role in combustion phasing and emissions, mainly throughout the local effect of heat losses on charge temperature. In addition to piston bowl geometry, pre-combustion chamber significantly helps to create the turbulence flow and internal swirl ratio throughout the combustion chamber. Most of the European diesel passenger cars are equipped with pre-combustion chamber diesel engines rather than direct injection engines because they have a better compromise between efficiency, noise and emissions [19]. Combustion system of these engines includes a main combustion chamber and a swirl flow pre-combustion chamber connected by a communicating passage. The communicating passage is connected tangentially to the pre-combustion chamber so as to induce consistent, repeatable swirling flow pattern gasses in the pre-combustion chamber during the compression stroke of the engine cycle. The swirl pattern thoroughly mixes the air, unburned and burned fuel in the pre-combustion chamber. However, the likelihood of new anti-pollution regulations will necessitate the use of HCCI-like combustion strategies. In order to use these technologies in HCCI mode, it is necessary to understand the impacts of pre-combustion chamber of diesel engines in HCCI-like modes. As expected, pre-combustion chamber can decrease the rapid pressure rise rate of HCCI combustion and consequently decreases the probability of knocking phenomenon. However, reviewed literature revealed that there is still lack of information on the effect of pre-combustion chamber on HCCI combustion. The present work aims to report further information by comparing two combustion chamber geometries (including with and without pre-combustion chamber) in HCCI combustion mode at the same operating conditions. Therefore, a single cylinder Ricardo diesel engine with Comet MK.V pre-combustion chamber, which was modified to natural gas fueled HCCI combustion engine, is adopted here to investigate the impact of pre-combustion chamber in HCCI combustion mode. Combustion process, engine performance and emissions are scrutinized for both combustion chambers.

2. Methodology

2.1. CFD model

The numerical simulation was performed using the AVL-FIRE software coupled with CHEMKIN solver for detailed chemistry calculation. The governing equations encompass the three basic laws of conservation, continuity and turbulence model equations. By coupling CFD code and CHEMKIN solver, the initial species concentration, pressure and temperature were provided by AVL-FIRE software to CHEMKIN solver. The chemical mechanism was implemented into CFD code to cover both combustion characteristics and emissions processes of HCCI combustion engine. This CFD code solves the average transport equation of total mixture mass, momentum and enthalpy. CHEMKIN code provided information on the new species and energy release after solving chemistry [20]. In order to investigate the combustion process of natural gas fueled HCCI engine, the GRI mech 3.0 chemical kinetic mechanisms which consist of 53 species and 325 reactions was used to describe the oxidation of the natural gas [21,22].

2.2. Combustion chamber geometry configurations

To study the effect of pre-combustion chamber, a new combustion chamber was created using CATIA software, which is schematically shown in Fig. 1. The volume of both chambers was kept constant in order to have the same constant compression ratio of 17.2. As shown in the modified combustion chamber in Fig. 1b, the top dead center (TDC) volume is slightly increased in order to compensate for the pre-combustion chamber volume. Details of the combustion chamber configurations are given in Table 1.

2.3. Computational domain

Due to the symmetrical geometry of both Ricardo Comet MK.V and the modified combustion chamber, FIRE Fame-Engine module was chosen to generate the computational grid for half of the combustion chambers. The choice of an average cell size is 0.8 mm and

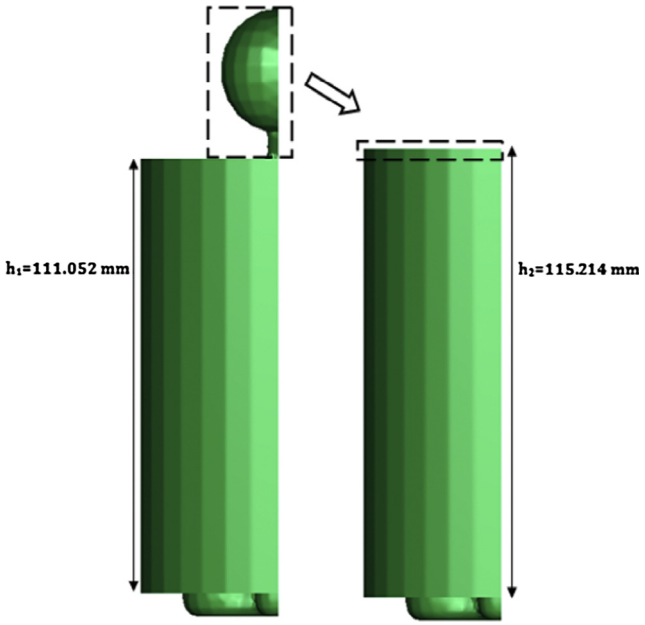

Fig. 1. Modification of the combustion chamber of Ricardo engine, (a) comet MK.V chamber, and (b) modified chamber.

Table 1
Configurations of the combustion chamber geometries.

Specifications	Comet MK.V	Modified
Swept volume (L)	0.5016	0.5016
Pre-chamber volume (L)	0.0167	–
TDC volume (L)	0.0143	0.031
Compression ratio	17.2	17.2
h (mm)	111.052	115.214

a time step of 0.2° crank angle degree (CAD) provided good numerical accuracies and computation stability. This resulted in 68,192 and 30,816 cells, respectively, for Comet MK.V and modified combustion chambers at TDC. The generated grids for both geometries at TDC are shown in Fig. 2. Due to the special shape of comet MK.V chamber, a large number of cells with small size are allotted to the pre-chamber (Fig. 2a) in order to provide good accuracy.

This paper investigates mainly the effect of pre-combustion chamber on combustion processes in the cylinder in a closed cycle, and the calculation range is considered from intake valve close (IVC) to exhaust valve open (EVO).

For initial conditions, all the cells in the domain were set to have a uniform initialization with a pressure of 2.7 bar and a temperature of 450 K at IVC. For boundary conditions, the meshes of the pre-combustion chamber and cylinder head were kept stationary, while that of the piston bowl was made a moving one. Walls temperature was set to 400 K in the simulation. The k–ε model was employed for modeling turbulence. At the beginning of the simulation, an amount of each species (air and fuel) is introduced to have a homogeneous air/fuel mixture. The mole fraction of CH_4, O_2 and N_2 under each equivalence ratio is shown in Table 2.

2.4. Engine experiments for model validation

Experimental data was obtained from a modified single-cylinder Ricardo E6/MS diesel engine coupled to a DC motoring/dynamometer. As shown in Fig. 2a, a cylinder head with a Ricardo Comet MK.V compression swirl combustion chamber is fitted in this engine. This type of combustion chamber possesses two parts. The swirl chamber in the head which has a spherical form and the lower half has a truncated cone which communicates with the cylinder by means of a narrow throat. The second part includes special cavities cut into the crown of the piston [24]. The compression ignition (CI) engine was modified to achieve HCCI engine combustion by introducing natural gas fuel in the intake manifold. The experimental setup is shown in Fig. 3. The engine was maintained at two constant speeds of 500 and 800 rpm and run with an open throttle. The intake system encompasses a 1 kW heater which is incorporated within the air meter casing. Intake air–fuel temperature was set at 400 K and is measured before the intake valve using a K-type thermocouple. The natural gas flow rate is measured using YAMATAKE flow meter and then is introduced to the intake manifold by a mixer which is located upstream of the intake valve to ease proper mixing. The engine out air fuel ratio (AFR) value is measured using a Lambda sensor which is installed in the exhaust manifold. A 1 kW electrical heater was used in the crankcase for to warm up the oil before starting. The oil temperature is maintained at 330 K.

A Fotek rotary encoder with a resolution of 0.1° CAD was mounted on the engine crankshaft to monitor the engine rotational speed and coordinate the pressure trace w.r.t crank position. Combustion pressure is measured with a piezo-electric AVL pressure transducer connected to an amplifier. A computer program was developed to analyze the experimental data. The intake pressure at IVC was taken as a reference point and changed by a supercharger from 2.2 to 3 bar. The basic engine specifications for the

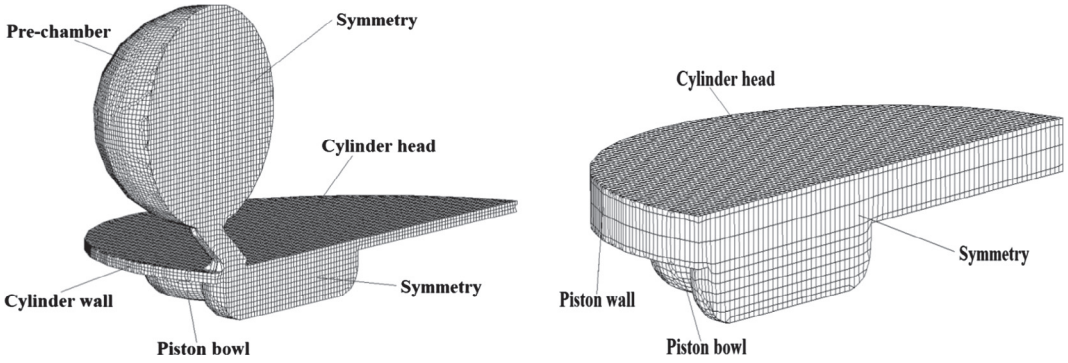

(a) Comet MK.V chamber (b) Modified chamber

Fig. 2. Computational meshes for both geometries at TDC, (a) comet MK.V chamber, and (b) modified chamber.

Table 2
Mole fraction of CH_4, O_2 and N_2.

Equivalence ratio	Mole fraction of CH_4 (%)	Mole fraction of O_2 (%)	Mole fraction of N_2 (%)
0.2	2.057	20.57	77.373
0.3	3.054	20.366	76.58
0.4	4.032	20.161	75.807
0.5	4.99	19.96	75.05

Table 3
Ricardo engine specifications.

Parameter	Specification
Engine type	Single cylinder E6/MS
Bore	76.2 (mm)
Stroke	110 (mm)
Displacement	501 (cc)
Compression ratio	17.2:1
IVC	36 (ABDC)
IVO	7 (BTDC)
EVC	7 (ATDC)
EVO	36 (BBDC)

current study are listed in Table 3. In order to achieve HCCI combustion, the Ricardo diesel engine is cold-started as CI mode. The engine warmed up in CI mode and when oil and water temperature reached 330 K, diesel fuel was cut-off and natural gas was induced by intake manifold to provide a homogeneous air–fuel mixture.

Six different operating conditions were selected from experiments done on natural gas fueled HCCI Ricardo engine. The operating conditions and uncertainty values for the engine parameters used in this study are, respectively, presented in Tables 4 and 5. Both motoring and combustion modes are considered with a wide range of intake pressure, while the intake temperature and

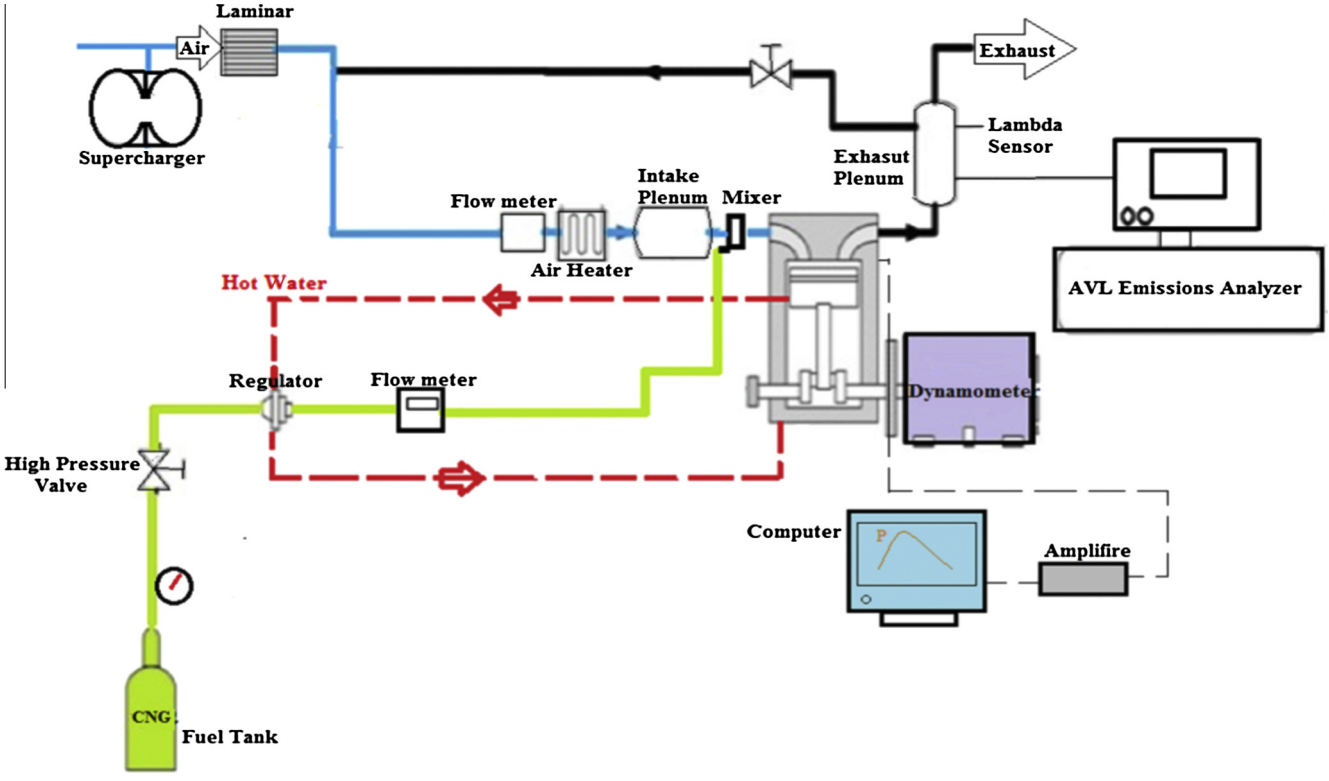

Fig. 3. Schematic diagram of the experimental HCCI setup.

Table 4
Ricardo operating conditions for the considered cases.

Case no.	Engine mode	P_{IVC} (bar)	T_{Inlet} (K)	Engine speed (rpm)	Equivalence ratio
1	Motoring	1.3	300	800	–
2	Combustion	2.2	400	800	0.3
3	Combustion	2.5	400	800	0.3
4	Combustion	2.7	400	800	0.3
5	Combustion	3	400	800	0.3
6	Combustion	2.7	400	500	0.3

Table 5
Experimental uncertainty.

Parameter	Uncertainty (%)
Temperature	<2
Pressure	<2
Engine speed	<1
Fuel flow rate	<1
Air flow rate	<1

equivalence ratio was kept constant. The experiments were carried out at two constant speeds of 500 and 800 rpm.

3. Results and discussion

3.1. Model validation

The six considered cases were used to validate the CFD model coupled with detailed chemical reaction mechanism under various engine operating conditions. Fig. 4 compares the numerical and experimental in-cylinder pressure for various cases. It is clear that during the whole part of the closed engine cycle, the calculated cylinder pressure traces almost matches the corresponding experimental ones. For all combustion mode cases, the highest discrepancy is seen during the expansion stroke. As shown in Table 6, the peak pressures discrepancy between the experimental and numerical results is less than 2.43%. Moreover, the discrepancy of the SOC [23] between the computation and experiment is less than 0.36%. There are two possible explanations for this result. The first is that the 3D CFD model is performed on the assumption that the mixture consists of fuel and air, residual gases are not considered in the simulation at the beginning of the calculation. However, as shown in Fig. 2a, due to the special shape of combustion chamber, a considerable amount of residual gases remain in the combustion chamber. Thus, the effect of residual gas on combustion characteristics is pronounced. The second possible explanation is that the mixture homogeneity is prefect in the numerical model, while in the actual HCCI combustion engine there are locations where temperature and mixture inhomogeneity exist throughout the combustion chamber.

In the following sub-sections, this validated model is used to compare the natural gas fueled HCCI engine with and without pre-combustion chamber at different air–fuel ratios. The case 4 of considered operating conditions in Table 4 is chosen as the base numerical conditions and various equivalence ratios (Φ = 0.2, 0.3, 0.4 and 0.5) are examined for considered combustion chambers around this point. Combustion, performance and emissions characteristics are analyzed in detail.

3.2. Cylinder pressure and heat release rate

To have a better understanding of the combustion process, the in-cylinder pressure and HRR versus crank angle for both

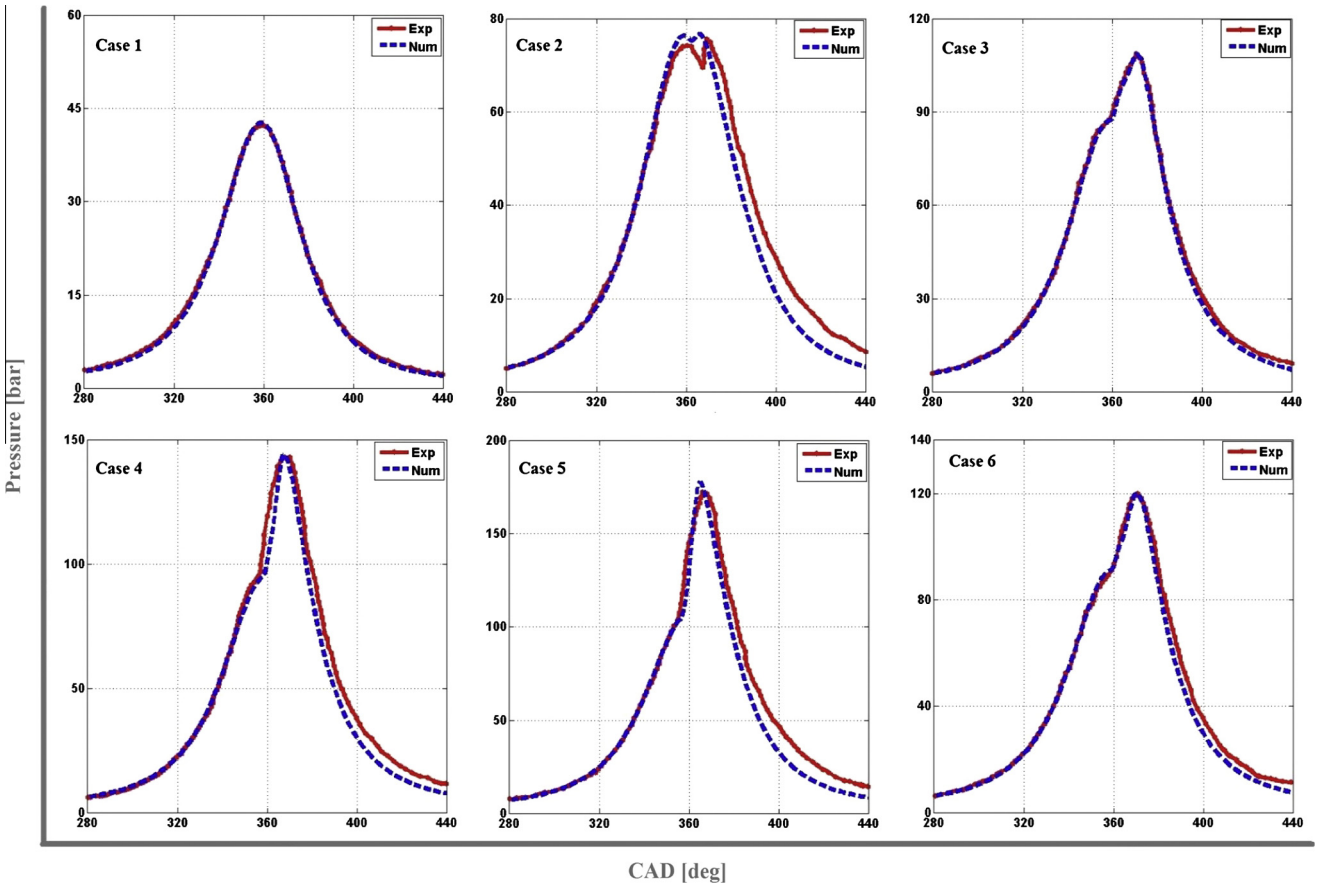

Fig. 4. Comparison of numerical and experimental combustion pressure.

Table 6
Comparison of experimental and numerical results for SOC and P_{max} at six considered cases.

Case	SOC–CFD (°CA ATDC)	SOC–Exp (°CA ATDC)	P_{max}–CFD (bar)	P_{max}–Exp (bar)	Error–SOC (%)	Error–P_{max} (%)
1	–	–	42.73	42.1	–	1.5
2	Misfiring	Misfiring	76.6	75.2	–	1.77
3	Misfiring	Misfiring	115.52	115.3	–	0.19
4	4.3	5.2	144.1	143.6	0.36	0.34
5	−0.6	−1.1	178.34	174.1	0.14	2.43
6	7.4	7.9	120.19	118.5	0.13	1.4

combustion chamber geometries are compared at equivalence ratio of 0.2 and 0.3. Fig. 5 compares the effect of pre-combustion chamber on the in-cylinder pressure and HRR. As can be seen, the modified chamber shows a higher in-cylinder pressure and HRR compared to comet MK.V chamber. With an equivalence ratio of 0.2, comet MK.V chamber experiences misfiring process, while modified chamber exhibits an enhancement of the combustion phasing. By modifying the combustion chamber geometry, the peak cylinder pressure and HRR increases and SOC is advanced. The positions of SOC [24] are presented in the figure. It can be seen that, with an equivalence ratio of 0.3, the highest peak of HRR (193.074 J/deg) appears at around 5° before top dead center (BTDC) for the modified chamber, while for the comet MK.V chamber, the HRR peak (59.849 J/deg) occurs at around 5° after top dead center (ATDC). Moreover, it is obvious that with the modified chamber, the HRR curve is narrower than that of comet MK.V. The modified chamber presents the faster ascending and descending of HRR. Therefore, it can be concluded that, with the modified chamber, speed of combustion is too fast so that natural gas fueled HCCI engine experiences shorter CD in comparison with comet MK.V chamber.

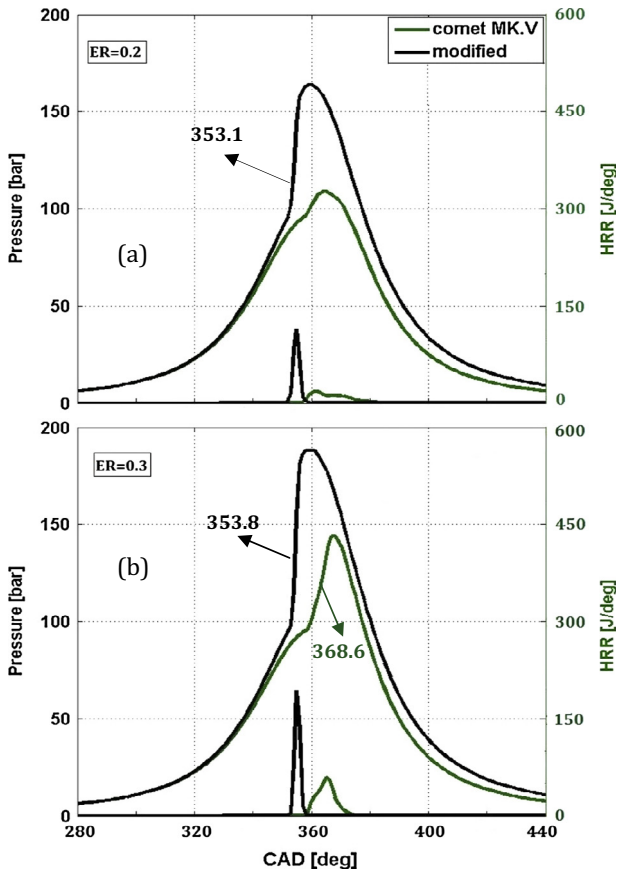

Fig. 5. The in-cylinder pressure and HRR at different equivalence ratios.

3.3. Engine performance

IMEP and output work per kg fuel are compared in Fig. 6 for both combustion chambers. As shown in Fig. 6a, HCCI engine experiences higher IMEP with the modified chamber compared to comet MK.V chamber. The maximum increase in IMEP (74.23%), occurred at an equivalence ratio of 0.2 where the HCCI engine with comet MK.V chamber tolerated the misfiring process whereas its

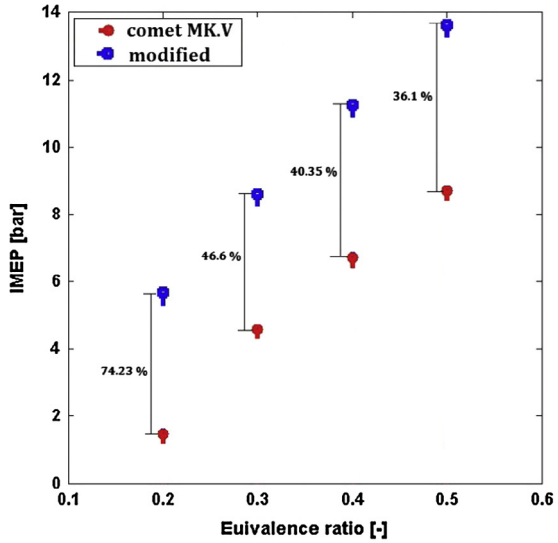

(a) IMEP

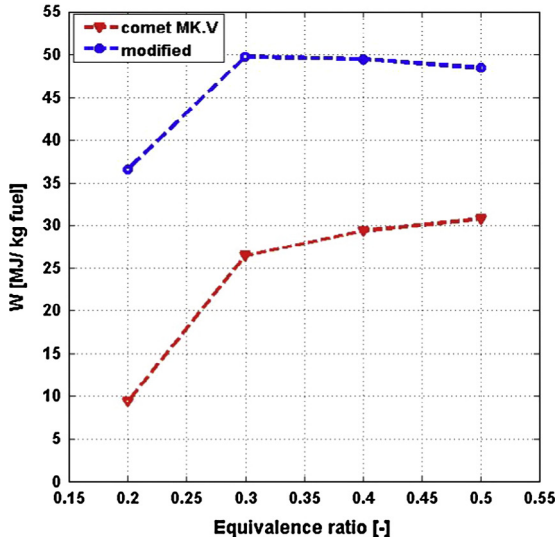

(b) Work

Fig. 6. Variation of IMEP and work for comet MK.V and modified geometries at different equivalence ratios.

counterpart experienced a complete combustion (Fig. 5a). The average increase in IMEPs with the equivalence ratio is 49.3%. It is also observed in this figure that, for both geometries the IMEP rises with the equivalence ratio.

Fig. 6b depicts the work done per cycle per kg fuel for both geometries at different equivalence ratios. Work done by the engine is calculated by integrating the area under the *P–V* curve. It is found that, the HCCI engine with comet MK.V chamber produces less work compared with modified chamber. This attributed to the fact that the compression and expansion pressure increased for the modified chamber (Fig. 5).

Because the engine work is negative during the compression stroke, the HCCI engine with the modified chamber performs more positive work during the expansion stroke, which increases the overall work during the entire engine cycle. The work done per kg of fuel is increased for the HCCI combustion with comet MK.V chamber with increasing the equivalence ratio. It can be seen in Fig. 6b that there is a slight decrease in the engine work per kg of fuel for the HCCI combustion with modified chamber for richer mixtures ($\Phi > 0.3$). The most likely reason for this result is that, the amount of available fuel in the cylinder increases by 24.4% and consequently the engine output work increases by 23.65% when increasing the equivalence ratio from 0.3 to 0.4. However, this decreases slightly the overall engine work per kg of fuel. The same trend occurs with an equivalence ratio of 0.5 for the HCCI combustion with the modified chamber.

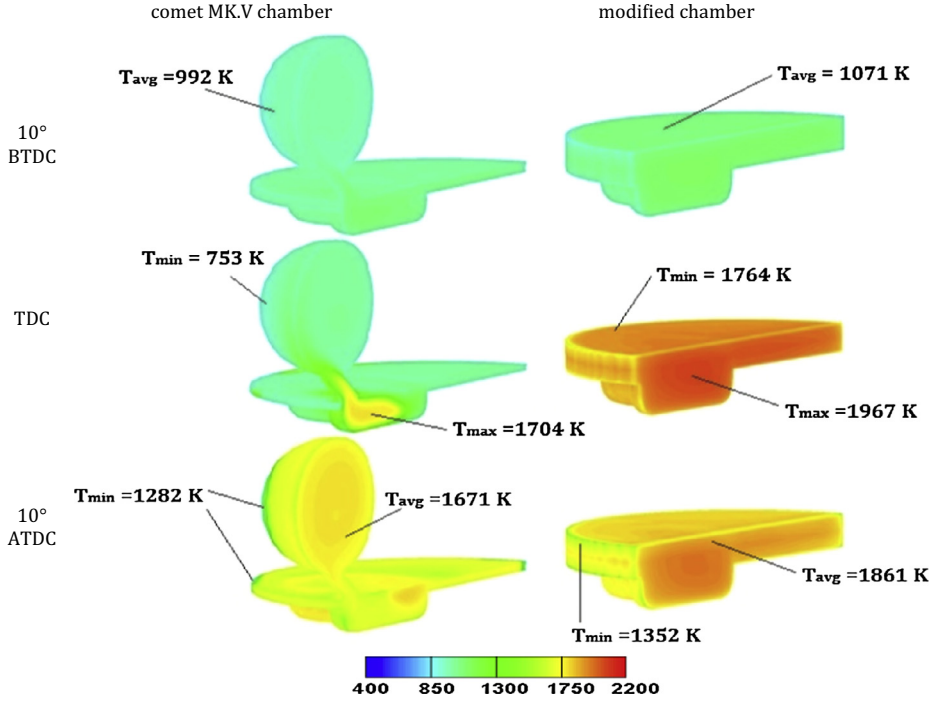

Fig. 7. Comparison of in-cylinder temperature at different crank angles.

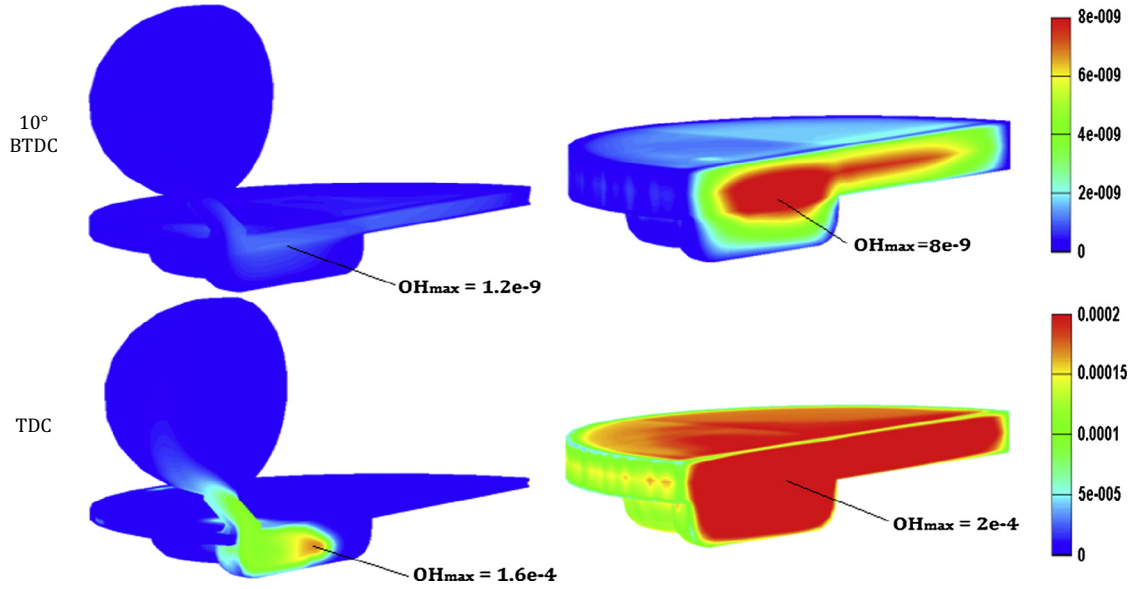

Fig. 8. Comparison of OH mass fraction at different crank angles.

3.4. Temperature and OH distribution

Fig. 7 shows the temperature distribution for comet MK.V and modified chambers at 10° BTDC, TDC and 10° ATDC, with an equivalence ratio of 0.3. As shown in this figure, the temperature for the HCCI combustion with modified chamber is higher than that of comet MK.V. This corroborates the findings presented earlier that the HCCI engine with modified chamber has a higher cylinder pressure, HRR and IMEP. For example, at 10° BTDC, the average temperature for the HCCI combustion with comet MK.V chamber is 992 K, while it is 1071 K for the modified chamber HCCI combustion. At TDC, it is observed that there is a considerable temperature inhomogeneity in the HCCI engine with comet MK. chamber. As shown in this figure, some zones in the pre-chamber experience minimum temperature of 753 K, while the maximum combustion temperature (1704 K) occurs in the center of main chamber. The ignition spot is located in the center of main chamber and the combustion propagates into the pre-chamber. It prevents the simultaneous ignition in the whole chamber. On the other hand, the temperature is nearly uniform in the HCCI engine with modified chamber. The minimum combustion temperature (1764 K) occurs near the cold wall boundary where there is heat transfer between the charge and the cylinder walls. It is also reveals that the difference between the minimum and maximum combustion temperature is low because numerous fuel mixture spots in the combustion chamber were ignited simultaneously which led to rapid HRR (Fig. 5). At 10° ATDC, for comet MK.V chamber, combustion expands considerably into pre-chamber and the average combustion temperature is 1671 K, while the combustion temperature average is 1861 K for the modified chamber. It can be concluded that, the HCCI combustion with comet MK.V decreases the combustion temperature on average and consequently diminishes the HRR. Therefore, it expands the operating range and reduces the likelihood of knocking phenomenon especially for richer mixtures ($\Phi > 0.3$).

Fig. 8 exhibits the OH concentration in the cylinder. OH is an ignition radical during the high-temperature reactions and the first ignition spot can be found from the distribution of OH concentration [25]. At 10° BTDC, the maximum OH mass fraction occurs in the center of modified chamber which indicates the initial ignition spot. At TDC, the maximum OH mass fraction occurs in the center of comet MK.V chamber main chamber where the combustion temperature is high (Fig. 7).

3.5. Pollutants formation

To examine the combustion features of HCCI engine with comet MK.V and modified chambers, NO, HC and CO emissions were predicted and compared at different equivalence ratios.

3.5.1. NO emission

Fig. 9a presents the combustion temperature and NO mass fraction at an equivalence ratio of 0.3 for both geometries. A direct proportional correspondence between the temperature and NO emission is observed in this figure. NO emission of HCCI engine with modified chamber is tangibly higher than that of comet MK.V. As demonstrated in Fig. 5 comet MK.V has longer HRR than the modified chamber. Since the total heat release is the same for both chambers at an equivalence ratio of 0.3 (Fig. 9b), the length of

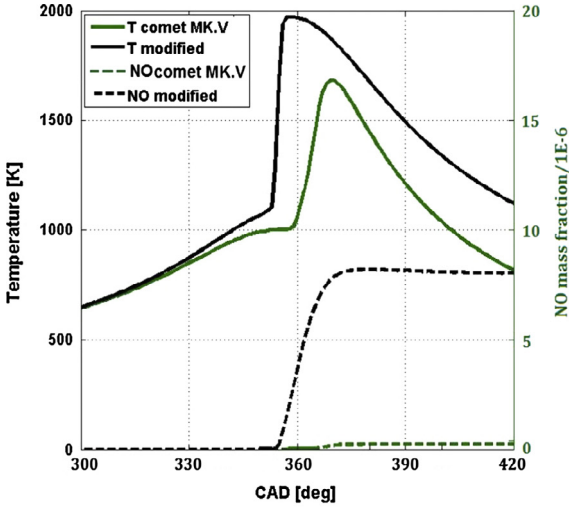

(a) Temperature and NO emission at ER=0.3

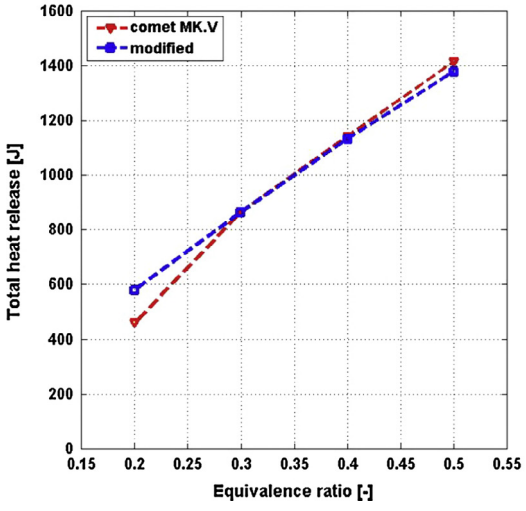

(b) Total heat release at different equivalence ratios

Fig. 9. (a) Temperature trace and NO concentration at equivalence ratio of 0.3; (b) Total heat release rate at different equivalence ratios.

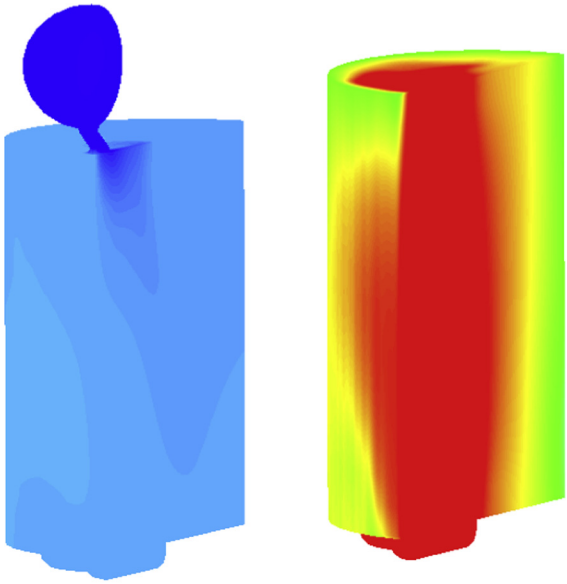

(a) comet MK.V (b) modified

Fig. 10. NO mass fraction for both chambers at EVO and ER = 0.3.

heat release process together with the low heat release value at each crank angle results in a long duration of low temperature combustion [26]. Subsequently, NO emission for the HCCI engine with comet MK.V chamber is lower than that of the modified chamber. Fig. 10 shows the NO distribution for both combustion chambers with an equivalence ratio of 0.3 at EVO. As expected, the HCCI engine with modified chamber generates higher level of NO emission compared with the HCCI engine with comet MK.V chamber. As shown in Fig. 10a, the minimum NO mass fraction belongs to the pre-combustion chamber where the temperature is lower. In contrast the minimum NO emission resides near the cylinder wall for modified chamber. Furthermore, the most of NO emission resides in the combustion chamber center where the temperature is the highest. Therefore, it can be concluded that the HCCI engine with comet MK.V chamber has a much lower NO emission compared to that with modified chamber.

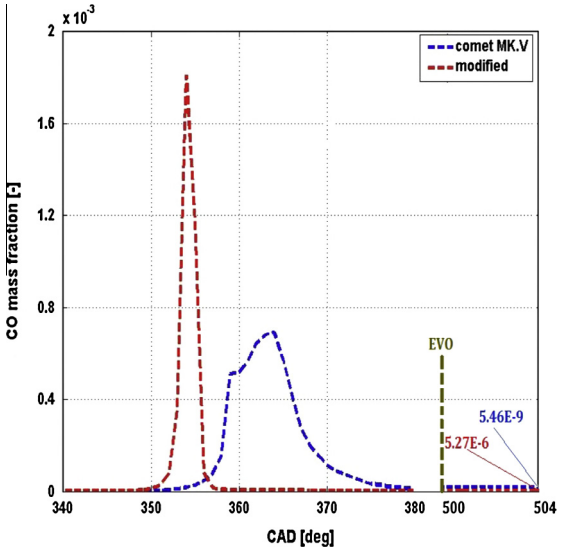

Fig. 11. CO emission history at ER = 0.3.

Table 7
CO and HC emissions in (kg/kg fuel) unite.

ER	$CO_{comet\ MK.V}$	$CO_{modified}$	$HC_{comet\ MK.V}$	$HC_{modified}$
0.2	0.177	2.24E−5	0.53	3.31E−9
0.3	0.0003	3.16E−7	8.17E−7	7.75E−14
0.4	4.6E-7	5.52E−7	4.27E−13	1.12E−13
0.5	7.89E-7	7.64E−7	4.4E−13	8.7E−14

3.5.2. CO and HC emissions

Fig. 11 shows the history of CO emission as a function of the crank angle for the HCCI engine with comet MK.V and modified chamber at an equivalence ratio of 0.3. For the modified chamber, CO is formed and oxidized quickly before TDC, while the formation and oxidation of CO is too long with comet MK.V chamber. It also reflects that the HCCI engine with modified chamber experiences a shorter CD compared to that of comet MK.V chamber. The mass fraction of CO emission for the HCCI engine with comet MK.V chamber is 5.27E−6 at EVO, while it is 5.46E−9 for the modified chamber.

Table 7 compares the level of CO and HC emission as a function of the equivalence ratio for both geometries. The emission of HC and CO is calculated in kg/kg fuel unit. It is observed that, the HCCI engine with modified chamber generates lower CO and HC emission compared to that with comet MK.V chamber. As shown in Table 7, the maximum level of CO emission for comet MK.V and modified chamber is 0.177 and 2.24E−5 kg/kg fuel which occurred at an equivalence ratio of 0.2. At an equivalence ratio of 0.2, the HCCI engine with comet MK.V chamber tolerates misfiring process which leads to a greater level of CO emission at EVO. In contrast, the HCCI engine with modified chamber experiences a complete combustion, thereby generating low level of CO emission. As shown in Fig. 12 and by comparing the HC emission (Table 7), it can be concluded that the majority of the HC emission resides in the pre-combustion chamber regions as a consequence of incomplete combustion. With an equivalence ratio of 0.2, the HCCI engine produces 0.53 and 3.31E−9 kg/kg fuel of HC emission with comet MK.V and modified chamber, respectively. Overall, it reveals the ability of the modified chamber to reduce CO and HC emissions which are ordinary pollutants in the HCCI combustion engines.

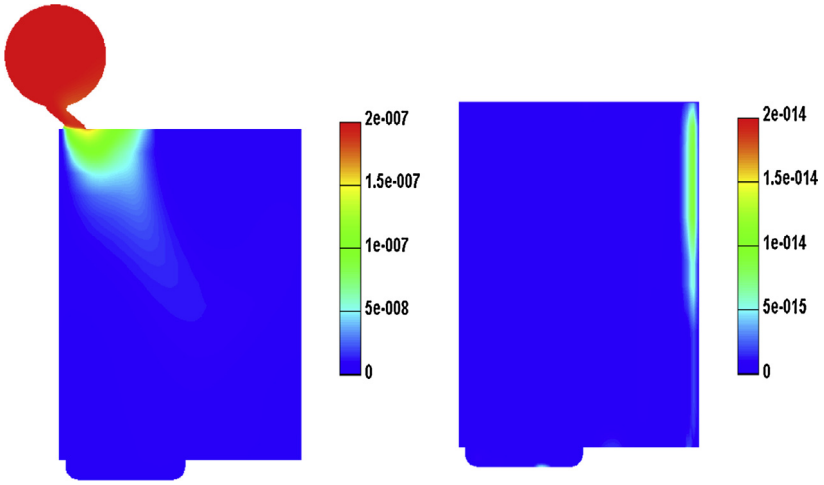

(a) comet MK.V (b) modified

Fig. 12. HC mass fraction for both chambers at EVO and ER = 0.3.

4. Conclusions

The present paper investigated the effect of pre-combustion chamber geometry on the combustion and emissions characteristics of natural gas fueled HCCI engine at different equivalence ratios using the coupled AVL-CHEMKIN CFD model. Both Comet MK.V and modified chambers were taken into consideration in this study. The comparison between both geometries were carried out in terms of in-cylinder pressure and HRR, engine performance (IMEP and work per kg fuel), temperature and OH mass fraction distributions and emissions at various equivalence ratios. The general conclusions can be summarized as follows:

- Higher combustion pressure and HRR are observed with the modified chamber and SOC position is advanced considerably compared to comet MK.V chamber. It can be inferred that the modified chamber experiences shorter CD in comparison with comet MK.V.
- The modified chamber has higher IMEP in comparison with comet MK.V chamber. Furthermore, the average increase in IMEPs with the equivalence ratio is 49.3%. The results revealed that, with the increase of equivalence ratio, the engine work per kg fuel increases for the HCCI combustion with comet MK.V chamber, while it adversely affects the engine work per kg fuel for the HCCI engine with modified chamber at richer mixtures ($\Phi > 0.3$).
- The HCCI engine with comet MK.V chamber decreases the combustion temperature average and consequently, decreases the HRR and pressure rise rate. It prolongs the operating range and reduces the likelihood of knocking process, especially for richer mixtures ($\Phi > 0.3$).
- The HCCI engine with modified chamber generates a higher level of NO emission compared to modified chamber. The maximum NO mass fraction for the modified chamber resides in the center of combustion chamber where the temperature is high. CO and HC emissions decreased substantially for the HCCI engine with modified chamber.

Finally, it can be concluded that, taking in to consideration the engine performance and emissions especially CO and HC emissions, the HCCI engine with modified chamber is preferred at low equivalence ratios ($\Phi < 0.3$).

References

[1] Bedoya Ivan D, Saxena Samveg, Cadavid Francisco J, Dibble Robert W, Wissink Martin. Experimental study of biogas combustion in an HCCI engine for power generation with high indicated efficiency and ultra-low NOx emissions. Energy Convers Manage 2012;53:154–62.

[2] Aceves SM, Flowers DL, Westbrook CK, Smith JR, Pitz W, Dibble R. A multi-zone model for prediction of HCCI combustion and emissions. SAE Paper 2000. 2000-01-0327.

[3] Zheng Junnian, Caton Jerald A. Effects of operating parameters on nitrogen oxides emissions for a natural gas fueled homogeneous charged compression ignition engine (HCCI): results from a thermodynamic model with detailed chemistry. Appl Energy 2012;92:386–94.

[4] Godino Jose Antonio Velez, Garcia Miguel Torres, Aguilar Fco Jose Jimenez-Espadafor, Trujillo Elisa Carvajal. Numerical study on HCCI combustion fueled with diesel oil using a multi-zone model approach. Energy Convers Manage 2015;89:885–95.

[5] Canakci Mustafa. Combustion characteristics of a DI-HCCI gasoline engine running at different boost pressures. Fuel 2012;96:546–55.

[6] Liu Haifeng, Zheng Zhaolei, Yao Mingfa, Zhang Peng, Zheng Zunqing, He Bangquan, et al. Influence of temperature and mixture stratification on HCCI combustion using chemiluminescence images and CFD analysis. Appl Therm Eng 2012;33–34:135–43.

[7] Treahima A, Ito N, Tojo T, Ijjim A, Yoshida K, Shoji H. A study of the effects of varying the compression ratio and fuel octane number on HCCI engine combustion using spectroscopic measurement. SAE technical paper 2013-32-9031, 2013.

[8] Tojo T, Yoshida K, Iijima A, Shoji H., et al. Analysis of the effects of a higher compression ratio on HCCI combustion characteristics using in-cylinder visualization and spectroscopic measurement. SAE technical paper 2012-32-0078, 2012.

[9] Vressner Andreas, Hultqvist Anders, Johansson Bengt. Study on combustion chamber geometry effects in an HCCI engine using high-speed cycle resolved chemiluminescence imaging. SAE Paper 2007. 2007-01-0217.

[10] Jung Dongwon, Lida Norimasa. Closed-loop control of HCCI combustion for DME using external EGR and rebreathed EGR to reduce pressure-rise rate with combustion phasing retard. Appl Energy 2015;138:315–30.

[11] Machrafi Hatim. Experimental validation of a kinetic multi-component mechanism in a wide HCCI engine operating range for mixtures of n-heptane, iso-octane and toluene: influence of EGR parameters. Energy Convers Manage 2008;49:2956–5965.

[12] Knop V, Boulerie J, Bohbot J, Jay S. Controlling CAI combustion mode with VVA: a simulation approach. SAE Paper 2007. 2007-01-0177.

[13] Weall A, Szybist J, Edwards K, Foster M, Confer K, Moore W. HCCI load expansion opportunities using a fully variable HVA research engine to guide development of a production intent cam-based VVA engine: the low load limit. SAE Int J Engines 2012;5(3):1149–62.

[14] Tandra V, Srivastava N, Soliman A. A discrete VVA-based phenomenological model of an HCCI engine. SAE Paper 2010. 2010-01-1240.

[15] Christensen M, Johansson B, Hultqvist A. The effect of combustion chamber geometry on HCCI operation. SAE 2002. 2002-01-0425.

[16] Liu H, Zhang P, Li Z, Zheng Z, et al. An investigation of different combustion chamber configuration, intake temperature, and coolant temperature in a HCCI optical engine. SAE technical paper 2011-01-1765, 2011.

[17] Yu R, Bai X, Vressner A, Hultqvist A, et al. Effect of turbulence on HCCI combustion. SAE technical paper 2007-01-0183, 2007.

[18] Jim_enez-Espadafor Francisco J, Garcia Miguel Torres, Herrero Jos_e A Correa, Villanueva Jos_e A Becerra. Effect of turbulence and external exhaust gas recirculation on HCCI combustion mode and exhaust emissions. Energy Fuels 2009;23:4295–303.

[19] Pinchon P. Three dimensional modeling of combustion in a prechamber diesel engine. SAE Technical Paper 1989;890666.

[20] AVL FIRE User Guide, Version 2011, AVL List Gmbh; 2009.

[21] Smith GP, Golden DM, Frenklach M, Moriarty NW, Eiteneer B, Goldenberg M, et al. GRI-mech3.0 data; 2006. <http://www.me.berkeley.edu/gri_mech.html>.

[22] Gharehghani A, Hosseini R, Mirsalim M, Yusaf T. A computational study of operating range extension in a natural gas SI engine with the use of hydrogen. Int J Hydrogen Energy 2015;40(17):5966–75.

[23] Ricardo E6/MS variable compression ratio, serial No. 126/76, Manual. Ricardo & CO., Engineers (1972) LTD. Shoreham-by-sea: Sussex; 1972.

[24] Kirchen P, Shahbakhti M, Koch CR. A skeletal kinetic mechanism for PRF combustion in HCCI engine. J Combust Sci Technol 2007;179:1059–83.

[25] Wang Zhi, Shuai Shi-Jin, Wang Jian-Xin, Tian Guo Hong. A computational study of direct injection gasoline HCCI engine with secondary injection. Fuel 2006;85:1831–41.

[26] Li J, Yang WM, An H, Maghbouli A, Chou SK. Effects of piston bowl geometry on combustion and emission characteristics of biodiesel fueled diesel engines. Fuel 2014;120:66–73.